REPORT DOCUMENTATION PAGE

Form Approved
OMB No. 0704-0188

1. REPORT DATE *(DD-MM-YYYY)*	2. REPORT TYPE	3. DATES COVERED *(From - To)*
	Technical Papers	

4. TITLE AND SUBTITLE

5a. CONTRACT NUMBER

5b. GRANT NUMBER

5c. PROGRAM ELEMENT NUMBER

6. AUTHOR(S)

5d. PROJECT NUMBER

5e. TASK NUMBER

5f. WORK UNIT NUMBER

7. PERFORMING ORGANIZATION NAME(S) AND ADDRESS(ES)

Air Force Research Laboratory (AFMC)
AFRL/PRS
5 Pollux Drive
Edwards AFB CA 93524-7048

8. PERFORMING ORGANIZATION REPORT

9. SPONSORING / MONITORING AGENCY NAME(S) AND ADDRESS(ES)

Air Force Research Laboratory (AFMC)
AFRL/PRS
5 Pollux Drive
Edwards AFB CA 93524-7048

10. SPONSOR/MONITOR'S ACRONYM(S)

11. SPONSOR/MONITOR'S NUMBER(S)

12. DISTRIBUTION / AVAILABILITY STATEMENT

Approved for public release; distribution unlimited.

DTSJ

FILE
6390RH65

MEMORANDUM FOR PRS (In-House Publication)

FROM: PROI (STINFO) 11 Jan 2001

SUBJECT: Authorization for Release of Technical Information, Control Number: **AFRL-PR-ED-TP-2001-006**
Bromaghim, D.R., et. al., "On-orbit Optical Observations of the ESEX 26kW Ammonia Arcjet"

Paper for the Journal of Propulsion and Power **(Statement A)**
(Deadline: N/A)

20020823 049

15. SUBJECT TERMS

16. SECURITY CLASSIFICATION OF:			17. LIMITATION OF ABSTRACT	18. NUMBER OF PAGES	19a. NAME OF RESPONSIBLE PERSON
a. REPORT	b. ABSTRACT	c. THIS PAGE			Leilani Richardson
Unclassified	Unclassified	Unclassified	A		19b. TELEPHONE NUMBER *(include area code)* (661) 275-5015

41 items enclosed

On-orbit Optical Observations of the ESEX 26kW Ammonia Arcjet

L.K. Johnson*, The Aerospace Corporation, El Segundo, CA

G.G. Spanjers†, D.R. Bromaghim‡, Propulsion Directorate, Air Force Research Laboratory, Edwards AFB, CA

M. W. Dulligan§, ERC, Inc., Air Force Research Laboratory, Edwards AFB, CA

Please make consistent throughout report

Abstract

During the course of eight flight firings of the ESEX 26-kW arcjet in March and April, 1999, optical observations from on-board and ground-based sensors were obtained. Images from the on-board still camera indicate that the nozzle temperature distribution is consistent with arcjet heating models and ground observations. Images of the thruster plume at 656 nm confirm predictions that the luminescent plume in the space environment is more diffuse and compact than the plume from a thruster operated in the laboratory at higher background pressure. Finally, observations using a ground-based telescope reveal a mixed greybody/line emission spectrum over the range 325-675 nm. The spectral features and line ratios are similar to those observed in ground-based measurements.

I. Introduction

Optical emission diagnostics were applied to the Electric Propulsion Space Experiment (ESEX), which operated successfully aboard the Advanced Research and Global Observation Satellite (ARGOS) in March and April, 1999. Two principal optical diagnostics were employed: an on-

---

* ESEX Chief Scientist, Member AIAA. Present address: Jet Propulsion Laboratory, 4800 Oak Grove Drive, Pasadena CA 91109, (818) 354-9878, lee.k.johnson@jpl.nasa.gov

† Project Scientist, Member AIAA.

‡ ESEX Program Manager, Member AIAA.

§ Project Scientist, Member AIAA.

Or "spectrograph" - same pg, next ¶ ?

board imager and a ground-based telescope/spectrometer. The primary objective of the imager was to provide visual confirmation of proper operation of the arcjet and to qualitatively observe transient phenomena. The secondary objective was to make quantitative measurements of the nozzle thermal distribution from radiance measurements and of the plume radiance distribution. The primary objective of the spectrograph was to prove the concept of ground-based spectral observations of low-flow, advanced thrusters (to compare ground test data to flight data) with a secondary objective of making high-resolution measurements to help determine frozen flow losses in the plume. In this paper we provide results from the flight experiment, draw conclusions, and point towards future efforts.

A major goal of the USAF Electric Propulsion Space Experiment (ESEX)[1] is to explore these above issues by making measurements on a high-power arcjet in flight. ESEX was launched on 23 February 1999 as 1 of 9 experiments aboard the USAF's Advanced Research and Global Observation Satellite (ARGOS).[2] The optical apparatus for ESEX consist primarily of an on-board still video camera and a ground-based spectrograph/telescope. Secondary optical sensors aboard the spacecraft include a pair of instrumented solar cells and a suite of four radiometers. Descriptions and results for the secondary sensors are given in detail by Spanjers et al.[3,4]

suggest spelling out

II. Video Camera

The video still camera consists of an optical train to focus and filter light from the arcjet, a CCD focal plane to capture the image, and associated electronics to control the camera and readout. The optical train consists of a heat-blocking filter and a narrow-band interference filter centered at 656 nm, which is the wavelength of the 3p-2s Balmer-alpha transition of excited atomic hydrogen. Laboratory studies of ammonia arcjets show that this wavelength dominates the visible plume. Although excited atomic hydrogen is a minor plume constituent, no other emission line in

Does this need to be identified for your audience?

the CCD range of sensitivity yields more information, and the Balmer-alpha line has been well studied in laboratory tests. The camera field of view is shown in Fig. 1. The focal plane consists of a 758 x 486 conventional CCD. An electronic shutter controls the CCD exposure to arcjet light; ground commanding is available to program each frame's exposure over the range 1/60 sec to 1/10,000 sec. The camera electronics unit reads and temporarily stores frames from the CCD. A maximum of 22 frames of video data may be stored in the camera electronics before readout, which functionally serves as a limit to the number of exposures possible during an arcjet firing.

III. Spectrograph/Telescope

The ground-based optical instrument consists of a spectrograph and CCD detector fed by one of the Air Force's telescopes on Maui. The telescope belongs to a joint Air Force Research Laboratory/Air Force Space Command unit and was made available on a visiting experimenter basis.[5] The telescope is located on Haleakala Crater, Maui, at an altitude of ~~almost exactly~~ approximately 10,000 ft. The pertinent optical elements consist of a 1.6 m diameter aluminized parabolic primary mirror, and a hyperbolic secondary mirror feeding a conventional Cassegrain focus of f/16 approximately 30" beyond a rear Blanchard mounting surface. A tertiary mirror is also available to direct light to a side Blanchard mount. The mount has ~~3~~ three axes of control, consisting of a conventional polar/declination astronomical arrangement mounted on top of an azimuth table. The telescope geometry is shown in Fig. 2.

MSSS ?

The ESEX instrument package mounted to the rear Blanchard surface (Fig. 3) consists of auxiliary optics, the spectrograph, the slit camera, and the CCD on the focal plane of the spectrograph. A schematic is presented in Fig. 4. On the way to the entrance of the spectrograph, light from the telescope passes through a filter wheel, where a Schott OG 550 orange filter is available for order sorting. No filters were used for the ESEX observations reported here. On the

same filter wheel is also a ground glass square. This square is rotated into the spectrograph field of view and illuminated by mercury and/or neon pencil-style emission lamps for wavelength calibration, which ensures that a properly diffuse target is in the field of view of the spectrograph. After the filter wheel, the f/16 converging beam passes through a doublet achromatic lens of 200mm focal length to f-match the beam to the f/7 spectrograph. Focusing of the telescope secondary is used to bring the image into focus on the entrance slit of the spectrograph.

The entrance slit is a custom assembly consisting of a slit or aperture, depending on application, piercing a plane polished reflecting surface. In a typical spectrograph application, the plane of the slit is normal to the incident light. In this case the plane of the mirrored entrance slit is angled 20 degrees about an axis parallel to the slit length. Consequently, light *not* entering the spectrograph is reflected at 40 degrees from the entrance axis towards a re-imaging lens consisting of a 50 mm focal length microscope objective. The converging beam leaving the microscope objective encounters a fold mirror and then strikes an intensified video-rate CCD focal plane. The secondary detector is used operationally in concert with telescope controls to ensure that the very small image is directed into the slit. The image on the spectrograph entrance slit is very small, approximately 50 microns in extent (which corresponds to less than a second of arc). The extra control afforded by the slit tracking camera is necessary to compensate for errors introduced by small inadequacies of the spacecraft orbital elements used to drive the telescope and for apparent image drift and oscillation due to atmospheric refractions.

An entrance slit of either slit or aperture format is used, depending on the application. Intensity calibrations do not require high wavelength resolution; rather, the intent is to capture an entire star image, including atmospheric position oscillation on the focal plane, for the total duration of the calibration exposure. A 600 micron aperture (approximately 10 arcsec) was found to be

satisfactory for this purpose; an aperture is preferred over a slit to reduce interference from background light. On the other hand, observations of the arcjet plume do require good resolution, and so a slit 50 microns (.8 arcsec) wide by about 10 mm high was employed, which proved to be a good balance between throughput and resolution. The narrow slit required the telescope operators' best efforts to continually direct the wavering image into the slit by making small adjustments to the telescope tracking.

The spectrograph itself consists of an Acton SP-500 non-imaging spectrometer. The plan for fulfilling the experiment objectives called for measurements at several different resolutions; the SP-500 includes a 3-grating interchangeable turret to facilitate remotely-controlled grating changes. The control box used to select gratings and rotate the grating to set the center wavelength was mounted on the telescope adjacent to the spectrograph and controlled *via* a cable and serial port from the remotely-located data acquisition computer. The spectrograph was modified slightly in several ways to optimize the integration, but the principal optical elements proved to be satisfactory for operation in any orientation (even inverted) in the factory configuration. The modifications performed include addition of an internal electronically controlled mechanical shutter just inside the entrance slit, addition of mounting holes in the base, and a tie-down for the movable exit fold mirror. The spectrograph was also purged continually with dry gaseous nitrogen.

The detector used consists of a Princeton Instruments back-illuminated, VISAR-coated, liquid nitrogen-cooled slow scan CCD with all-orientation dewar. The CCD format is 330 pixels along the slit axis by 1100 pixels along the wavelength axis; the pixel size is 25 microns. This CCD affords good sensitivity, on-chip binning, and very low noise. Performance trades indicated that this LN CCD would provide better signal/noise than an intensified CCD.

The detector controller is mounted on the telescope adjacent to the spectrograph. This control unit passes CCD data over a proprietary serial interface to the remotely-located data acquisition computer. The data acquisition computer itself is about 65 feet from the telescope base, but the extra cable necessary for the telescope cable management system to allow for unrestricted mount motion required approximately 160 feet of cabling. Several other displays are provided to the experimenter at the data acquisition computer desk. These include video displays of mount parameters, finder telescope image, and slit tracking camera image.

In practice, nightly observing runs consist of equipment checks, mount position calibration, wavelength calibration, focus adjustment, and data acquisition runs for either star intensity calibrations or arcjet firings. For star tracks, the RA/DEC catalog position of the calibration star is input to the mount computer, the mount is set to follow the sidereal motion, and the star is observed on the 30 arc-minute finder telescope display. The star image is in general not observed immediately on the slit tracking camera, and so the mount position is then biased while continuing to track sidereally, to direct the image onto the tracking camera and then into the slit. For satellite tracks, the mount computer reads a two-line element set and tracks in so-called "ballistic") mode. Both tracking modes incorporate the ability to continuously improve their automated tracking using real-time operator bias input. For satellite tracks, the azimuth table of the telescope is generally rotated so that the telescope's polar axis is more or less perpendicular to the satellite's path. This allows the tracking motion to be principally in the polar axis, which mimics an astronomical track (for which the mount structure and stability is optimized).

For arcjet firing observations, a dry run of the mount track was performed prior to the actual track and for some runs background sky data were acquired during this dry run pass. For other

tracks, the mount positions corresponding to the acquisition times of good data files were recorded, and then the mount was directed to the same positions soon after the satellite track was complete for backgrounds. A communications net was maintained among the ESEX operators at Kirtland AFB and the telescope/spectrograph operators at MSSS. This net allowed operators to be certain the arcjet was on when tracks were being attempted and facilitated inter- and intra-site operations.

IV. Observations and Analysis

During the spring, for descending node passes at night (given ARGOS' orbit), the spacecraft is not illuminated by the sun at MSSS rise. Further, operational constraints prevented arcjet starts before rise (for the available passes) ~~and so~~ therefore, the telescope track either had to be started in the blind or with assistance from an AF radar nearby. Both radar tracking and blind tracking worked well in practice, but blind tracking required ESEX personnel to coordinate and provide the best available element set to MSSS.

The spring of 1999 also proved to be problematic from a weather standpoint. Most nights during the available interval were unsatisfactory by MSSS' ~~usual~~ standards, due to cloud layers above the observatory, and for many nights, the observatory was shrouded in fog. The small number of clear nights and the arcjet battery charging cycle schedule ~~together~~ limited the observation opportunities considerably. Star calibrations were performed during the clear nights when the arcjet was not available and during arcjet track nights, as appropriate, when not preparing for the track.

Preliminary star calibration data for the wavelength range 320-670 nm using a 150 lpmm grating were obtained using the star Feige 110. The calibration ~~is~~ derived does compensate for

spectrograph and detector variations and atmospheric losses as a function of wavelength, but not as a function of elevation angle. A better calibration, including the elevation effect, will be derived in future work, but for elevations over 50 degrees the preliminary calibration should be accurate to +/- 15%. The approximately 10x loss in sensitivity towards the UV is approximately half due to grating blaze and half due to greater atmospheric attenuation in the UV.

Do you need this second "approx"?

Unfortunately, the weather and battery problems combined to preclude nearly all observations of the arcjet firing. However, firing 5 was successfully observed at approximately 2:50 a.m. local time on March 26, which was a night with thin high clouds. For this pass, the ¾ moon was setting at about 1 degree elevation at 288 degrees in the northwest. The pass geometry involved a maximum elevation of about 83 degrees at 286 degrees azimuth, so that the included angle between the moon and spacecraft was about 82 degrees, which unfortunately allowed the moon to illuminate the high clouds, producing a significant background.

Needs to be spelled out three-quarter

Fourteen exposures of the pass during the arcjet firing were obtained; of these, the first ten show structure associated with arcjet operation. Early in the pass, the arcjet, located ~~in~~ on the ram surface of ARGOS, is visible, but later in the pass, the body of ARGOS obscure the arcjet nozzle and plume. The last four exposures occur during the period when the nozzle and plume are obscured. The spectrograph was set to record a 320-670 nm wavelength range with a 150 lpmm grating blazed at 500 nm. The signal observed during the firing is large and consists of continuum radiation from the hot nozzle body peaking to the red of 670 nm along with discrete emission lines observed from 325 nm to 650 nm. Each exposure where arcjet signals were unambiguously recorded is shown in Figs. 5 and 6, and a summary of pertinent arcjet parameters for this firing is shown in Fig. 7. The exposure figure reveals that the arcjet was stably operating by the time data were obtained, ~~and~~ as the pass progressed, the signal stayed about the same until the last few

exposures where the nozzle and plume are progressively becoming obscured by the spacecraft body. Note that the vertical scale for Fig. 4 is relative energy, which represents partial use of the preliminary star intensity calibration.

The emission lines observed correspond to the Balmer series and the NH (A-X) molecular electronic transition, as expected, along with a number of smaller, less distinct structures. The results show many of the same features as high-power ammonia arcjet emission spectra taken earlier.[6]

Suggestion, unless it changes what you are trying to say.

The Balmer series is visible up to n=9, and no other transitions are seen in the Balmer limit region. The series terms become less intense as the degree of excitation increases, which is consistent with previous observations of high- and low-power arcjets. The other large signal ~~that~~ is observed is the NH (A-X) complex, whose central peak and wings constitute transitions involving different vibrational and rotational states within this electronic transition. In ground tests, both the Balmer series and the NH manifold have been compared to equilibrium conditions using Boltzmann temperature analysis. It is our intent in future work to carry out similar analyses to the extent they are practicable. The smaller structures observed around 355 nm have not been identified, although some similar (though not identical) features associated with N_2 (C-B) and N_2^+ (B-X) do show up in ground test data taken previously by the present authors in support of ESEX, as shown in Fig. 8.

An analysis was done to scale the continuum radiation to a blackbody energy distribution using temperature as a variable parameter. The results of this fit are shown in Fig. 9 for the exposure with the best statistics. The best fit temperature is 1842 K; this can be compared to a measured maximum nozzle temperature in ground test of 2100 K. It is not surprising that the flight data

show a lower temperature since thermal radiation from hot and cooler parts of the nozzle contribute to the continuum signal.

The on-board camera revealed plume emission and heated nozzle glow as expected. A series of images acquired as the arcjet heated up is provided in Fig. 10. The camera signals correlate well to plume emission and nozzle body temperature model predictions as well as previsouly measured nozzle thermal distributions.

V. Summary and Conclusions

Optical emission diagnostics, both on-board and remotely-based, were applied to the flight of the ESEX arcjet. The on-board imaging camera showed that plume emission and heating follow expectations and ground test data, where valid. The remote spectroscopic measurements proved the concept of ground-based measurements of low-flow advanced thruster plumes. The spectroscopic data reveal continuum and emission structure related to that seen in ground tests.

VI. Acknowledgements

The authors acknowledge the inputs from the TRW/RRC team in the design and characterization of the flight sensor package and ground-based thruster measurements, especially the efforts of Andy Hoskins. In addition, significant design and integration of the spectrometer package was obtained from the USAF Maui optical site team, including the contributions of Jack Albetski in particular.

VII. References

1. Bromaghim, D.R., LeDuc, J.R., Salasovich, R.M., Zimmerman, J.A., Matias, D.C., Sutton, A.M., Spanjers, G.G., Fife, J.M., Hargus, W.A, Spores, R.A. , Dulligan, M.J., Engelman, S.F., Schilling, J.H., White, D.C., and Johnson, L. K, "An Overview of the On-Orbit Results from the ESEX Flight Experiment," AIAA 99-2706, June, 1999. Also submitted to this issue, J. Prop and Power.

Please spell out to be consistent w/ other references. or abbreviate the others.

last name first

2. B.J. Turner, and F.J. Agardy, "The Advanced Research and Global Observation Satellite (ARGOS) Program," AIAA 94-4580, Sept. 1994.

3. Spanjers, G. G., Schilling, J. H., Bromaghim, D. B., Johnson, L. K., "Radiometric Analysis from the ESEX 26 kW Ammonia Arcjet Flight Experiment," submitted to this issue, Journal of Propulsion and Power.

4. Schilling, J. H., Spanjers, G. G., Bromaghim, D. B., and Johnson, L. K., "Solar Cell Degradation during the ESEX 26 kW Ammonia Arcjet Flight Experiment," submitted to this issue, Journal of Propulsion and Power.

5. AMOS User's Manual, Phillips Laboratory, 1996.

6. Hoskins, W.A., "High Power AJ Spectroscopy Analysis," Final Report, Olin/RRC 30 kW Arcjet Analysis, 1996.

- Note in text (pg 2; 2nd ¶; bottom), you list Spanjers for Ref. 3 + 4
- Need to list Ref 4 with Spanjers name first
  or put "Schilling, et al. [4]" in text

FIGURE CAPTIONS

Figure 1. ESEX thruster (right) and video still camera field of view. Ram direction is up.

Figure 2. MSSS 1.6 m telescope and three-axis mount.

Figure 3. ESEX spectrograph package mounted to the 1.6 m MSSS telescope.

Figure 4. Schematic diagram of ESEX spectrograph, detector, and slit camera.

Figure 5. Series of emission spectra from ESEX arcjet showing continuum radiation from the nozzle and line structure from the plume.

Figure 6. Spectrum obtained during arcjet firing well after nozzle is obscured by spacecraft body (The above is 10^{th} in the series, for comparison to Fig 5). Blackbody emission is gone but emission lines from the plume persist.

Figure 7. Arcjet parameters for Firing 5. Second line shows when observations from spectrograph were obtained.

Figure 8. Small unidentified emission structure as seen in ground and flight tests.

Figure 9. Blackbody fit to arcjet nozzle emission.

Figure 10. Series of images acquired from the on-board video camera showing the ramp to full power.

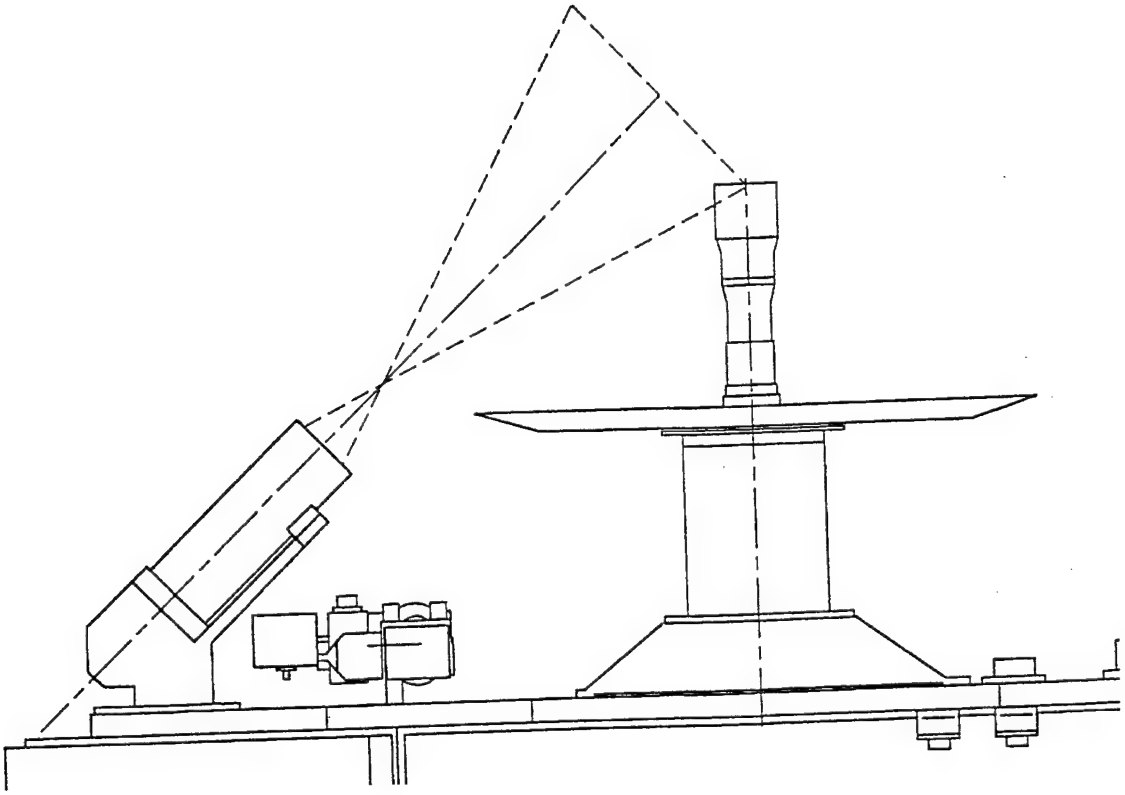

Johnson et al., Journal of Propulsion and Power, Fig. 1 of 10

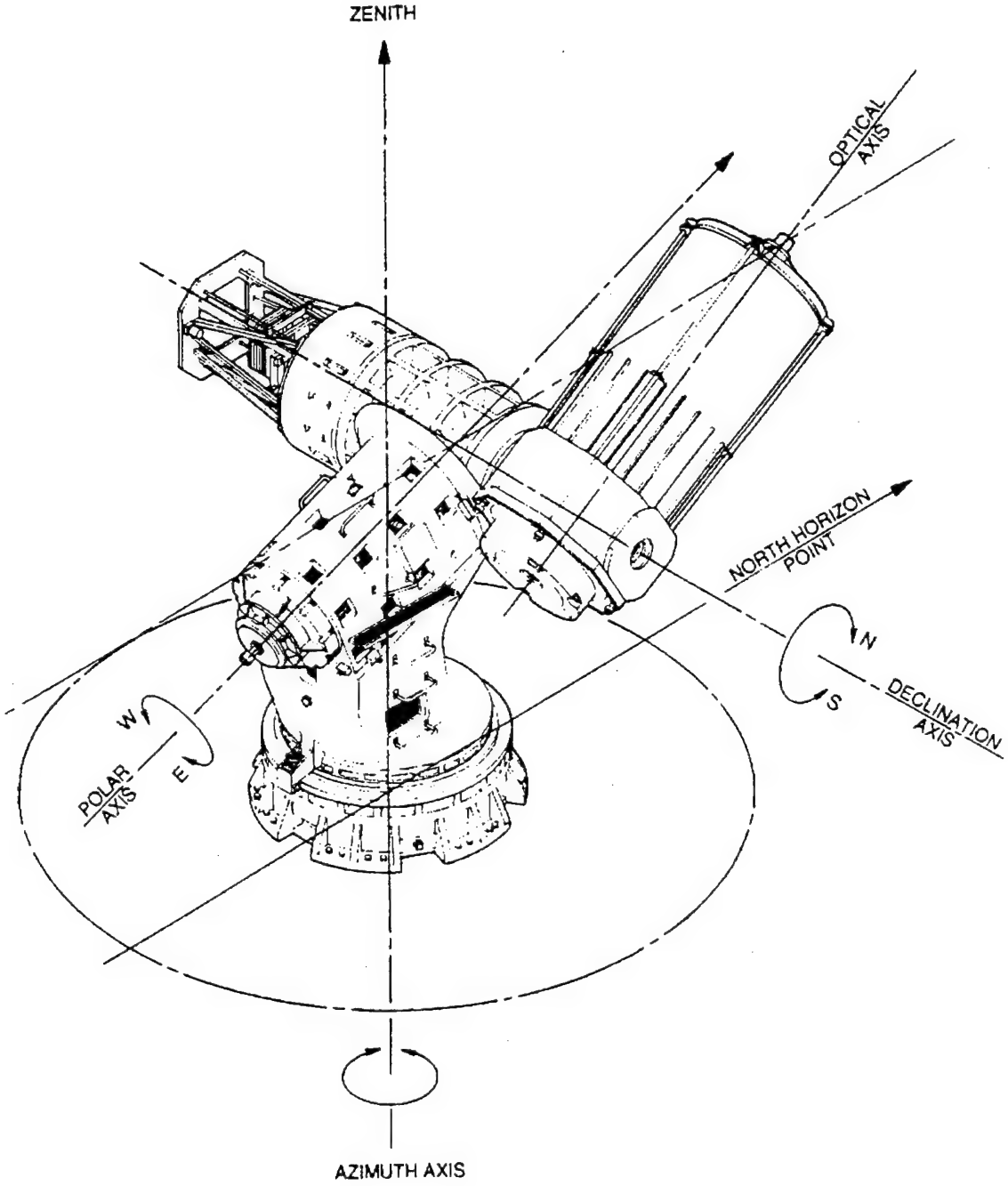

Johnson et al., Journal of Propulsion and Power, Fig. 2 of 10

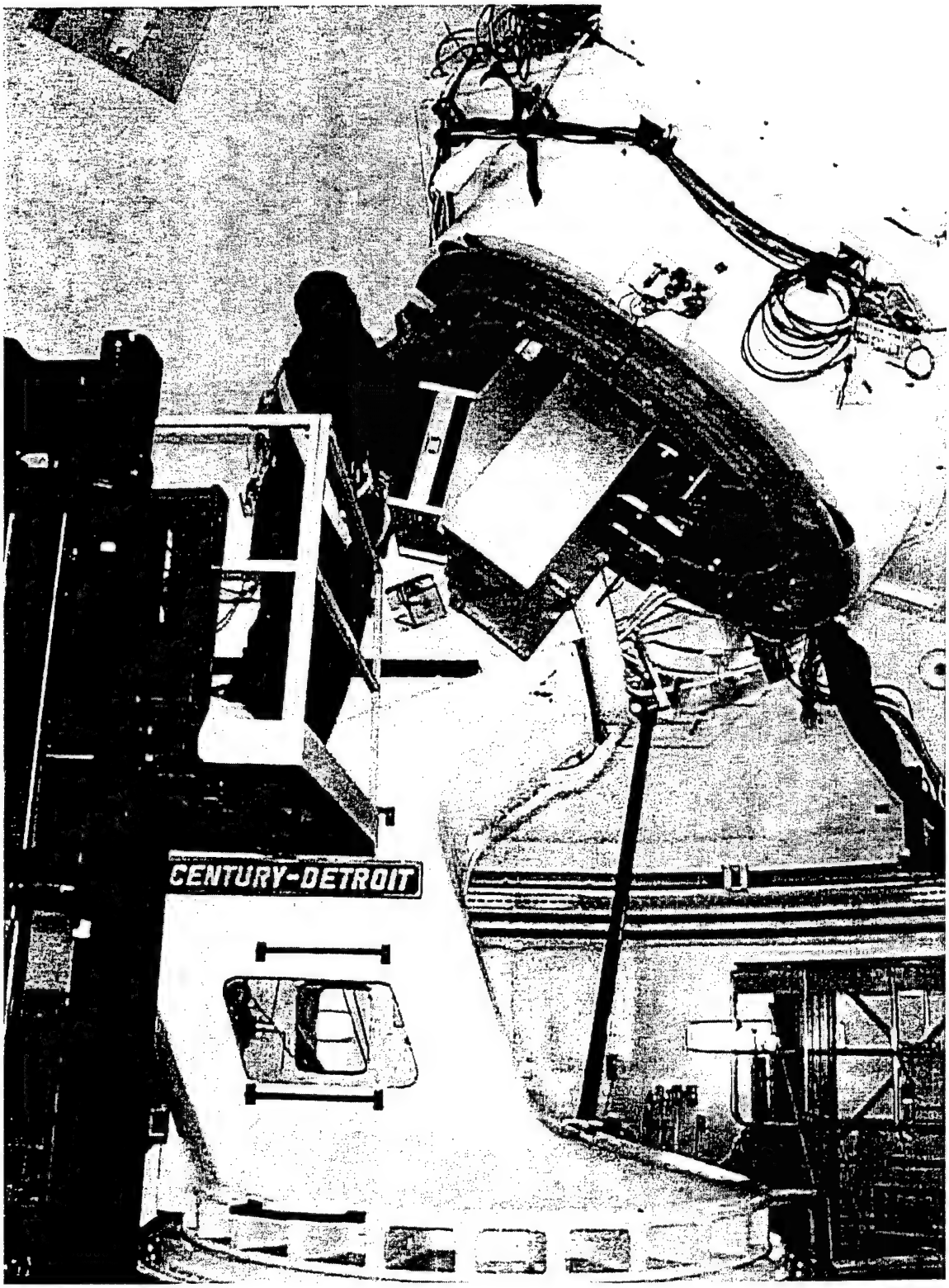

Johnson et al., Journal of Propulsion and Power, Fig. 3 of 10

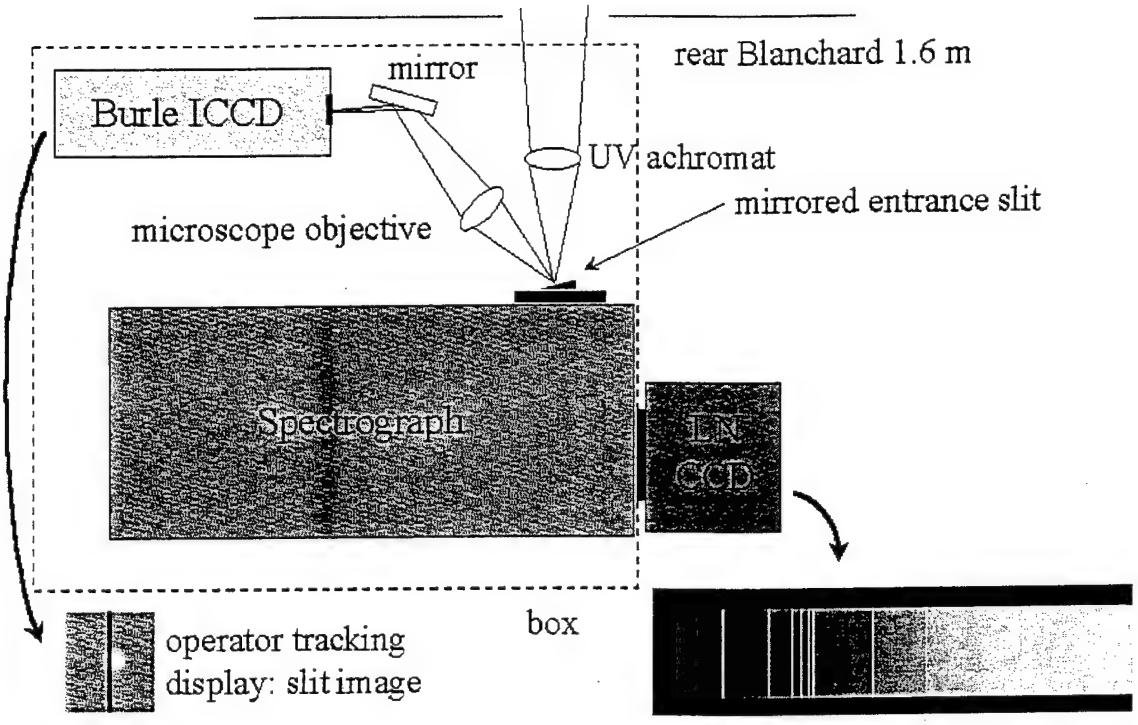
rear Blanchard 1.6 m
mirror
Burle ICCD
UV achromat
mirrored entrance slit
microscope objective
Spectrograph
I.N
CCD
box
operator tracking
display: slit image

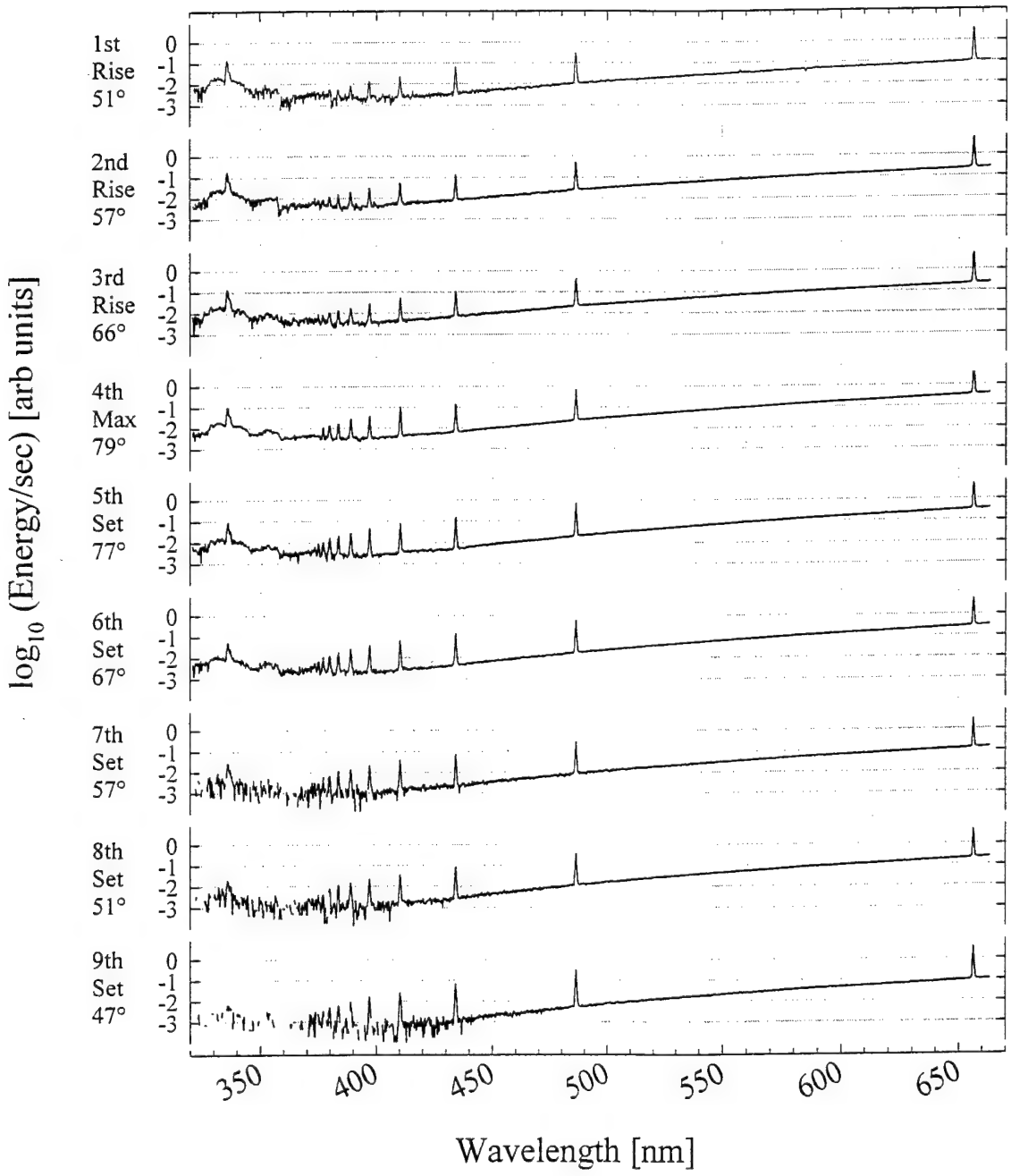

Johnson et al., Journal of Propulsion and Power, Fig. 5 of 10

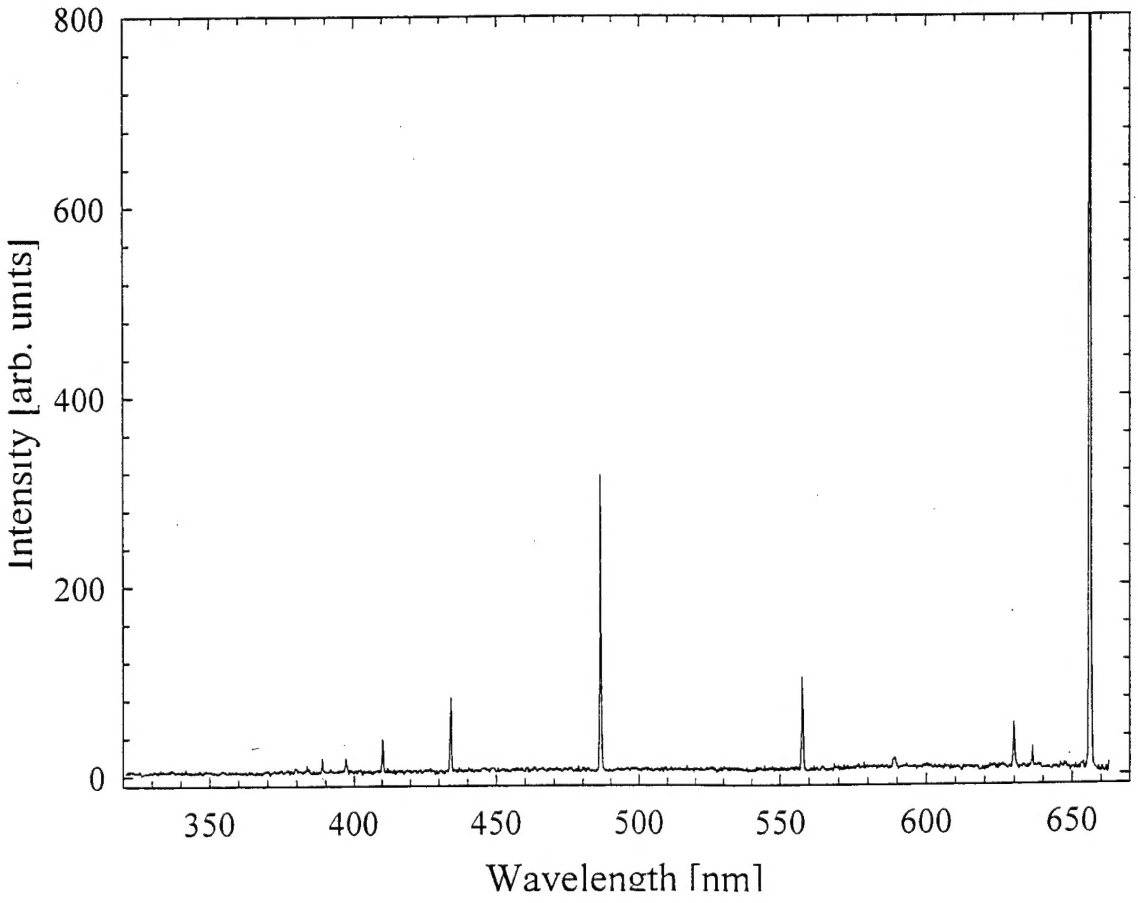
800
600
400
200
0
Intensity [arb. units]
350
400
450
500
550
600
650
Wavelength [nm]

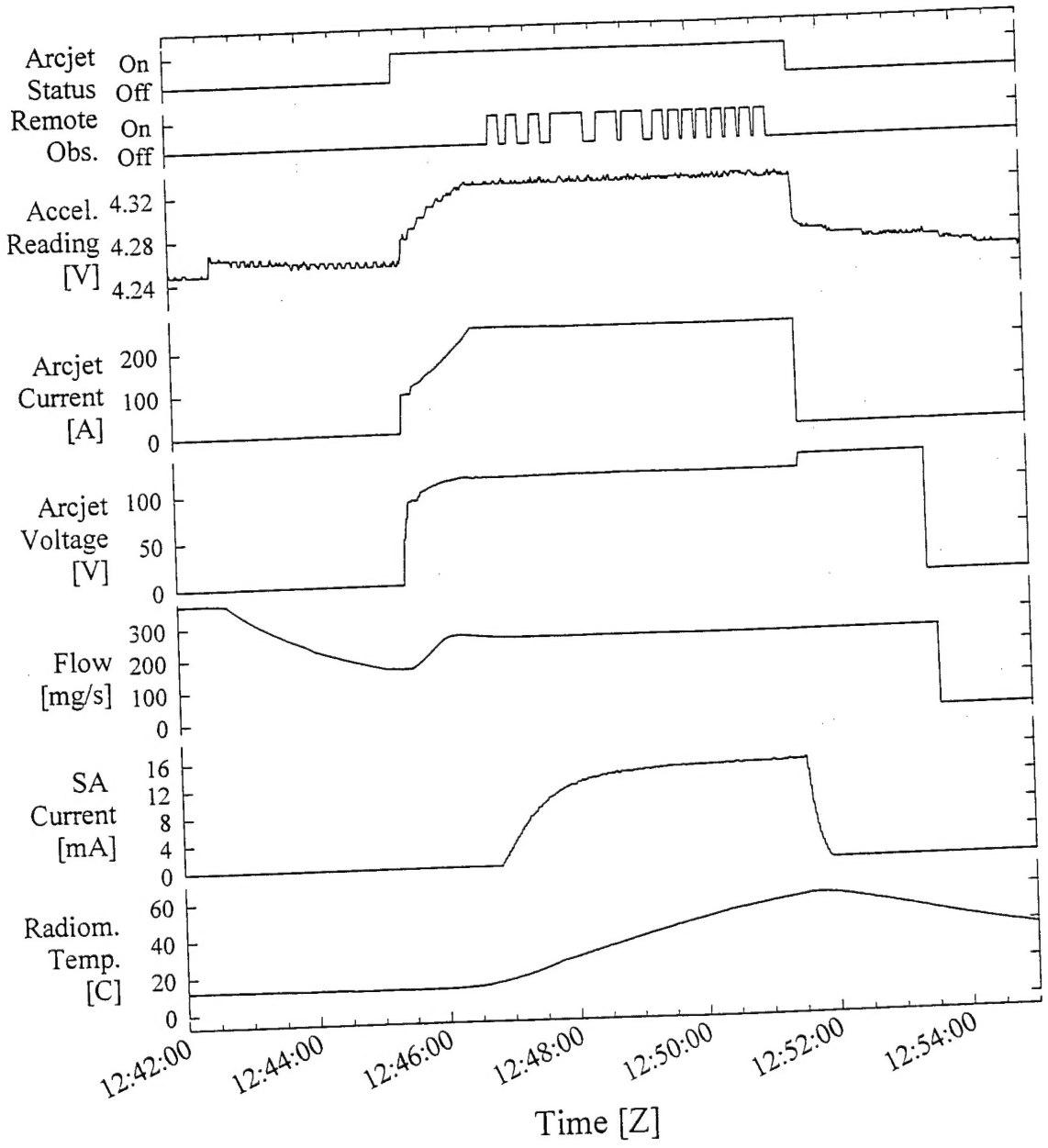

Johnson et al., Journal of Propulsion and Power, Fig. 7 of 10

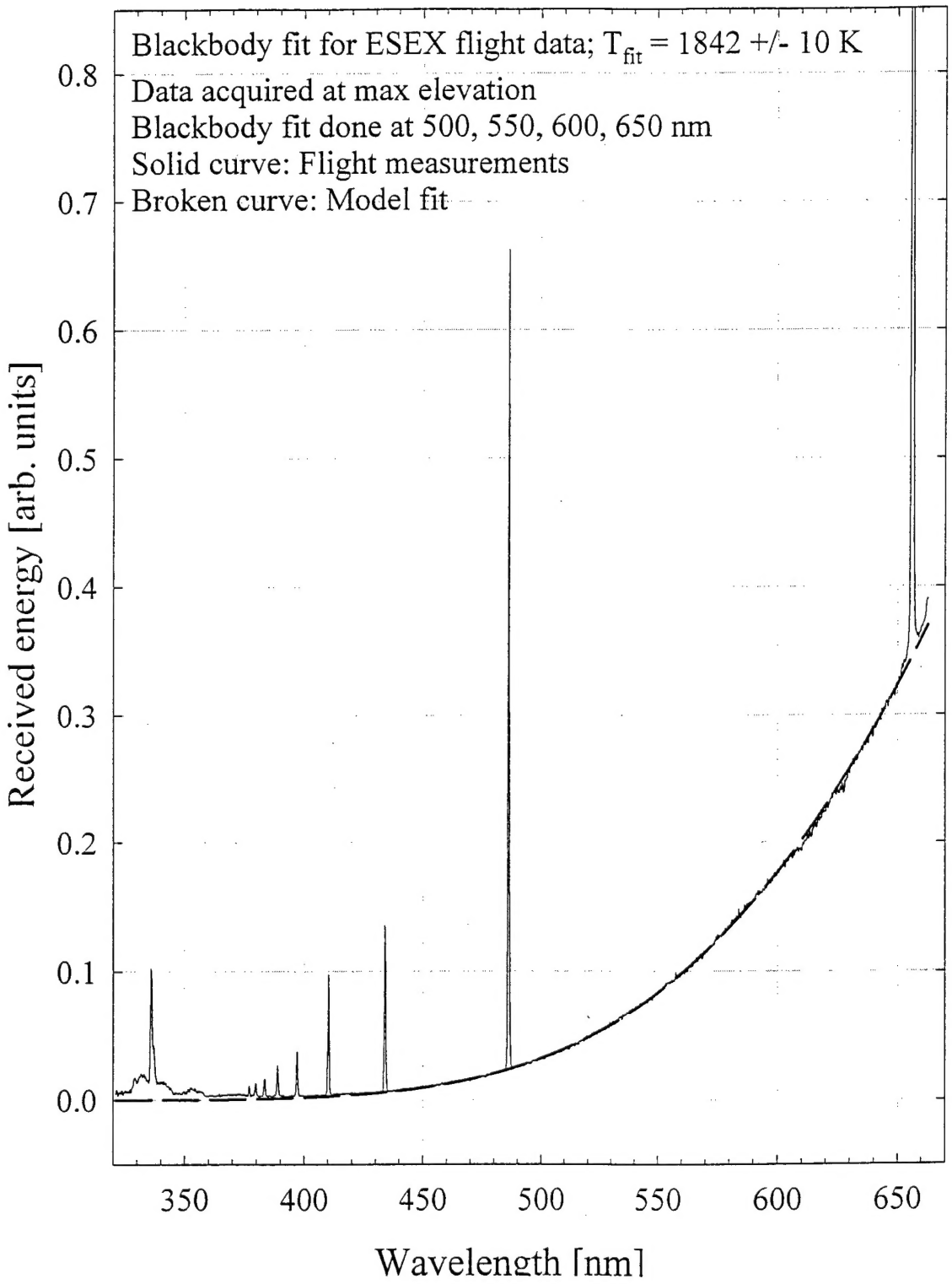

Johnson et al., Journal of Propulsion and Power, Fig. 9 of 10

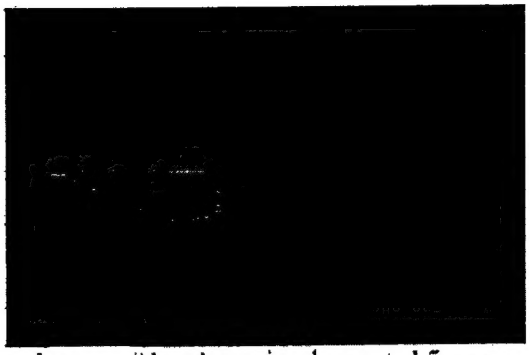

Image #1 - Acquired at t + 15 sec

Image #3 - Acquired at t + 45 sec

Image #2 - Acquired at t + 30 sec

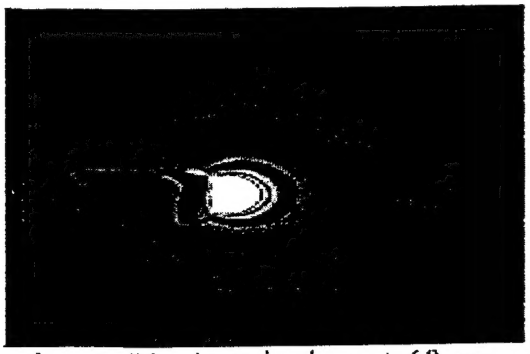

Image #4 - Acquired at t + 60 sec